Applied Thermal Engineering 55 (2013) 61–68

Contents lists available at SciVerse ScienceDirect

Applied Thermal Engineering

journal homepage: www.elsevier.com/locate/apthermeng

The effects of electronic controlled steam injection on spark ignition engine

İdris Cesur [a], Adnan Parlak [b,*], Vezir Ayhan [a], Barış Boru [a], Guven Gonca [b]

[a] Sakarya University, Technical Education Faculty, 54100 Sakarya, Turkey
[b] Yildiz Technical University, Naval Architect and Maritime Faculty, 34349 Besiktas, İstanbul, Turkey

HIGHLIGHTS

- We developed electronic controlled steam injection system for a SI Engine.
- Steam is injected into the cylinder during inlet period.
- Corrosive side effects are eliminated as steam is injected in the superheat form.
- Performance and specific fuel consumption are improved with the system.
- NO significantly decreased as steam homogenously mixed with gasoline–air mixture.

ARTICLE INFO

Article history:
Received 12 September 2012
Accepted 13 February 2013
Available online 19 March 2013

Keywords:
SI engine
Steam injection
Two-zone combustion model
Engine performance
Exhaust emissions

ABSTRACT

In this study, the effects of steam injection at different injection rates on the evaluations of performance parameters and emissions of a gasoline engine have been investigated. Electronically controlled steam injection method has been used to inject the steam into the engine. The optimum steam ratio has been determined as 20% of fuel mass (S20) in terms of performance and emission parameters. Steam injected gasoline engine has been modeled by using zero-dimensional two-zone combustion model for optimum steam ratio at full load condition. The obtained results have been compared with conventional gasoline engine in terms of performance and NO, CO, CO_2, HC emissions. The results of theoretical combustion model agree with experimental data quite well. In the experimental results, it is seen that the engine torque and the effective power increase up to 4.65% at 3200 rpm, specific fuel consumption reduces up to 6.44% at 2000 rpm. There is 40% average reduction in NO emissions at 2800 rpm and it is 31.5% in HC emissions at 2000 rpm.

1. Introduction

Pollutant emissions are occurred from engines due to lack of stoichiometric combustion of Hydrocarbon (HC) based fuels. It is known that the most effective, hazardous and heavy emissions in the exhaust gases are carbon monoxide (CO), hydrocarbons (HC), NO_x and particulate matter (PM) [1]. In recent years, significant measures have been taken on air pollution caused by automotive engines. One of the measures is water injection into the engine and it has been widely used in order to improve combustion efficiency and exhaust emissions. The usage of water in automobile engines has several benefits. Previous research has shown that it has significant impact on decreasing the peak flame temperatures and thereby reducing the NO_x emissions [2–4]. It has also been shown that introducing water into the cylinder may improve atomization and mixing [5,6]. Atomization and mixing improvement leads to increase in the combustion efficiency.

Based on improvement of combustion efficiency, Lif ve Holmberg [7] claimed that a finer atomization of the fuel during injection is carried out because of very low interfacial tension between fuel and water during to compression process, higher contact area is resulted in much better mixing of the air and fuel during the burning process.

Wang et al. [1] stated that the injected water causes to division of the fuel much more droplets with micro explosions. The combustion efficiency and engine performance improve with respect to reduction of the droplet diameter and increment of the total surface area of the droplets. Yoshimoto et al. [8] state that micro explosions of water content fuels improve brake efficiency and reduce pollutant emissions. They found that the kinematic viscosity

* Corresponding author. Tel.: +90 212 3832940; fax: +90 212 3832941.
E-mail addresses: aparlak@yildiz.edu.tr, adnanpar@gmail.com (A. Parlak).

1359-4311/$ – see front matter © 2013 Elsevier Ltd. All rights reserved.
http://dx.doi.org/10.1016/j.applthermaleng.2013.02.020

of the fuel is important factor affecting the micro explosions. Micro explosions increase with the kinematic viscosity of the fuel leading to improved performance and pollutant emissions parameters. Canfield [6], claimed that improved mixing also helped reduce NO_x and carbon emissions forming in the diffusive burning portion of the combustion process. Hang et al. [9], indicated that water-containing fuels are better atomized than pure hydrocarbon fuels, using high speed cameras.

In the literature, although so many studies are performed on water injection into (DI) diesel engine, there is not so much study on water injection into (SI) spark ignition engines. Lanzafame, carried out a theoretical and experimental investigation on water injection into intake air using a single cylinder spark ignition engine which has variable compression ratios. It expressed that there is considerably reduction in NO_x emissions when water injected into the engine at different mass ratio of fuel [10]. Subramanian et al. [11] performed an experimental investigation on effects of water injection into intake manifold of a single cylinder and hydrogen-fueled engine on performance and NO emissions. In the results, it is shown that the effective power and thermal efficiency increase at all injection ratios. NO emissions reduce from 7500 rpm up to 2490 rpm.

Based on literature reviews, water injection into gasoline and diesel engine has certain effects to reduce emissions and improve performance parameters. However, the water inside the cylinder cause to pronounced corrosion. Steam injection is the preferred method recently, in order to reduce this negative effect in the internal combustion engines [12–15], Ayhan, experimentally investigated the effects of steam injection into intake manifold of a diesel engine. According to the results obtained, NO_x emissions reduce up to 33%, effective power and torque increase up to 3% and SFC decrease up to 5% at 20% steam injection rate as a result of full load tests [12–15].

In this study, in order to prevent the effects of corrosion caused by water, steam injection is performed phase into intake manifold of the SI engine, on the back of the inlet valve and during the intake period. The steam is injected into the engine at rate of 10%, 20% and 30% of fuel mass. The experimental results obtained are given in comparison with the results of zero-dimensional-two-zone combustion model developed.

2. Material and method

2.1. Experimental set-up

The experiments were carried out with “Lombardini” SI engine. Table 1 and Fig. 1 shows the engine specification and schematic order of the experimental apparatus, respectively. So as to measure brake torque, the engine is coupled with an electric dynamometer of 20 kW absorbing capacity using an “S” type load cell with the precision of 0.01 kg.

In this study, MRU Spectra 1600 L type gas analyzer was used so as to measure exhaust emissions. The gas analyzer gives the amounts of CO, CO_2, NO, NO_x and HC emissions in (%) and ppm.

Table 1
Specification of the test engine.

Engine type	Lombardini
Bore [mm]	72
Stroke [mm]	62
Cylinder number	2
Stroke volume [l]	0.505
Power [kW]	15
Compression ratio	10.7
Cooling type	Water
Fuel system	Injectors

The uncertainty levels of the calculated parameters with respect to the measured ones, which are important for verifying the correctness of the test results, are shown in Table 2.

In order to carry out the steam injection into the engine, electronically controlled steam injection system has been developed. Steam has been obtained by means of exhaust waste heat from waste heat boiler. Steam in the waste heat boiler, which is kept in the form of saturated water with conditions of 3 bar and 133.5 °C, was injected with injectors which are positioned at the back of intake valve in the manifold. In the experiments, 10%, 20% and 30% steam ratios of fuel mass were used. Fig. 2 shows solenoid steam injectors fitted with suction manifold.

In order to measure inside cylinder pressure, AVL brand GH13Z-24 model, SI piezo-electric sensor and Kistler 5011B type charge amplifier was used in engine cylinder. SMETEC brand data card which has 1 Mbyte data signaling rate from single channel “Combi Combustion Indication System” was used for data transfer, and Heidenhain ROT426 type encoder which has 3600 pulse/revolution was used in order to measure angular position.

Experiments were done at variable engine speeds 1600, 2000, 2400, 2800, 3200 and 3600 rpm and full load condition. In order to compare, firstly standard SI engines tests were performed with gasoline fuel. Then the steam was injected at different mass ratios of fuel, into intake manifold when intake valves were opened during the suction period. The experiments were repeated for each steam ratios, performance and emission values were measured and compared with those of standard engine.

2.2. Theoretical model

The combustion simulation of spark ignition engine is carried out by using two-zone combustion model to calculate emissions, efficiency and power. The burned and unburned gas regions are divided by region border. In the cylinder, the equation of the energy conservation in differential form could be expressed as:

$$m\frac{du}{d\theta}+u\frac{dm}{d\theta}=-\frac{dQ_b}{d\theta}-\frac{dQ_u}{d\theta}-P\frac{dV}{d\theta}-\frac{dm_l}{d\theta}h_l \tag{1}$$

where m_l and h_l are leak mass and enthalpy of leak mass respectively. The first term of the left side of the equation is the internal energy rate and the second term is the mass rate depending on crank angle. The heat transfers from burned and unburned zone are expressed, respectively as:

$$\dot{Q}_b = h_{tr}A_bT_{bw} \tag{2}$$

$$\dot{Q}_u = h_{tr}A_uT_{uw} \tag{3}$$

where $T_{uw}=T_u-T_w$ and $T_{bw}=T_b-T_w$, h_{tr} is heat transfer coefficient of burned and unburned gas zones, A_b and A_u are the areas of burned and unburned gas inside the cylinder which are in contact with the cylinder walls and T_b, T_u and T_w are the temperatures of the burned gas zone, unburned gas zone and cylinder walls [16]. The change of stroke volume depending on crank angle:

$$\frac{dV}{d\theta}=\frac{\pi}{8}B^2S\sin\theta\left[1+\varepsilon\frac{\cos\theta}{(1-\varepsilon^2\sin^2\theta)^{\frac{1}{2}}}\right] \tag{4}$$

In order to solve the differential equations, the following expressions are used in the model. Internal energy:

$$\frac{du}{d\theta}=C_p-\frac{Pv}{T}\left(\frac{\partial\ln v}{\partial\ln T}\right)_P\frac{dT}{d\theta}-v\left[\frac{\partial\ln v}{\partial\ln T}+\frac{\partial\ln v}{\partial\ln P}\right]_T\frac{dP}{d\theta} \tag{5}$$

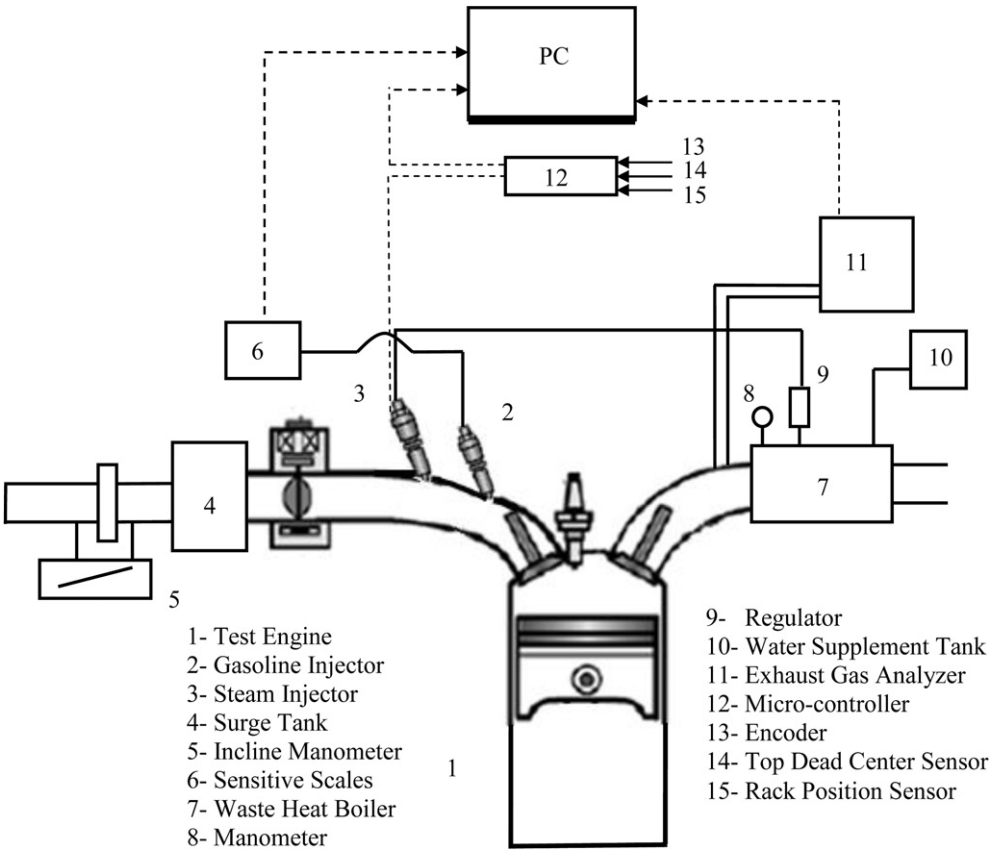

Fig. 1. Schematic order of the experimental apparatus.

The burned gas leaking through the rings:

$$\frac{dm_l}{d\theta} = \frac{Cm}{\omega} \tag{6}$$

where C and ω are blowby coefficient and angular velocity, respectively. The mass balance inside the cylinder can be expressed as:

$$m = m_a + m_f \tag{7}$$

where m_a and m_f are the masses of the air and fuel respectively. If the Eq. (7) is written in differential form, it becomes:

$$\frac{dm}{d\theta} = \frac{-Cm}{\omega} \tag{8}$$

Differential equation systems used in the calculation of the processes that consist during the period from the beginning of the compression to the end of the expansion process are given in Eqs. (14)–(19) [17].

The time (crank angle)-dependent expressions of pressure, burned and unburned gas temperatures, work, heat leak and heat loss are given respectively as:where x, A_{cyl} are the burning fraction

Table 2
The errors in parameters and total uncertainties.

Parameters	Systematic errors, ±
Load, N	1.0
Speed, rpm	1.0
Time, s	0.1
Temperature, °C	1.0
Fuel consumption, g	0.1
NO_x,	5% of measured value
CO, %	5% of measured value
HC, ppm	5% of measured value
Smoke, %	1
Parameters	**Total uncertainty, %**
Specific fuel consumption, g/kWh	1.2
Brake torque, Nm	0.7
Brake power, kW	1.0
Effective efficiency, %	1.3

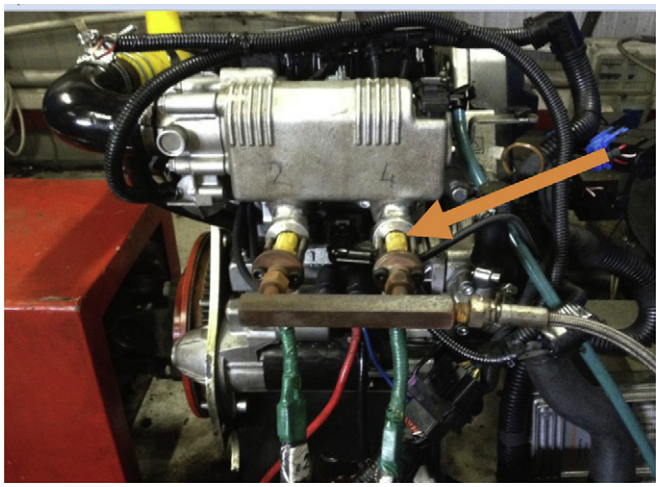

Fig. 2. Injector slot placed in the suction manifold and steam injector fitted with injector slot.

$$\frac{1}{m}\left(\frac{dV}{d\theta}+\frac{VC}{\omega}\right)+h_{tr}\frac{A_{cyl}}{\omega m}\left(\frac{\nu_b}{C_{p,b}}\frac{\partial \ln \nu_b}{\partial \ln T_b}\sqrt{x}\,\frac{T_b-T_w}{T_b}+\frac{\nu_u}{C_{p,u}}\frac{\partial \ln \nu_u}{\partial \ln T_u}\left(1-\sqrt{x}\right)\frac{T_u-T_w}{T_u}\right)$$

$$\frac{dP}{d\theta}=\frac{-(\nu_b-\nu_u)\,\frac{dx}{d\theta}-\nu_b\frac{\partial \ln \nu_b}{\partial \ln T_b}\frac{(h_b-h_u)}{C_{p,b}T_b}\left[\frac{dx}{d\theta}-\frac{(x-x^2)C}{\omega}\right]}{x\left[\frac{\nu_b^2}{C_{p,b}T_b}\left(\frac{\partial \ln \nu_b}{\partial \ln T_b}\right)^2+\frac{\nu_b}{P}\frac{\partial \ln \nu_b}{\partial \ln P}\right]+(1-x)\left(\frac{\nu_u^2}{C_{p,u}T_u}\left(\frac{\partial \ln \nu_u}{\partial \ln T_u}\right)^2+\frac{\nu_u}{P}\frac{\partial \ln \nu_u}{\partial \ln P}\right)} \tag{9}$$

and heat transfer area of the cylinder. $C_{p,b}$, $C_{p,u}$; ν_b, ν_u; h_b, h_u are specific heat at constant pressure, specific volume and specific enthalpy for the burned and unburned zones respectively.

$$\frac{dT_b}{d\theta}=-\frac{h_{tr}A_{cyl}\sqrt{x}(T_b-T_w)}{\omega m C_{p,b}x}+\frac{\nu_b}{C_{p,b}}\frac{\partial \ln \nu_b}{\partial \ln T_b}\frac{dP}{d\theta}+\frac{(h_b-h_u)}{xC_{p,b}}\left[\frac{dx}{d\theta}-\left(x-x^2\right)\frac{C}{\omega}\right] \tag{10}$$

$$\frac{dT_u}{d\theta}=-\frac{h_{tr}A_{cyl}(1-\sqrt{x})(T_u-T_w)}{\omega m C_{p,u}(1-x)}+\frac{\nu_u}{C_{p,u}}\frac{\partial \ln \nu_u}{\partial \ln T_u}\frac{dP}{d\theta} \tag{11}$$

$$\frac{dW}{d\theta}=P\frac{dV}{d\theta} \tag{12}$$

$$\frac{dH_l}{d\theta}=\frac{Cm}{\omega}\left[\left(1-x^2\right)h_u+x^2h_b\right] \tag{13}$$

$$\frac{dQ_l}{d\theta}=\frac{h_{tr}}{\omega}A_{cyl}\left[\sqrt{x}(T_b-T_u)+\left(1-\sqrt{x}\right)T_u-T_w\right] \tag{14}$$

Hohenberg [18] gives the coefficient of the heat transfer (h_{tr}) as:

$$h_{tr}=C_1V^{-0.06}P^{0.8}(xT_b+(1-x)T_u)^{-0.4}\left(\overline{S}_p+C_2\right)^{0.8} \tag{15}$$

where $\overline{S}_p$ is mean piston velocity in meters per second, $C_1=130$ and $C_2=1.4$ respectively.

Wiebe function states the burn fraction and x versus crank angle is used to express the heat release from combustion and determined as [19]:

$$x=1-e^{-a_v\left(\frac{\theta}{\theta_b}\right)^{(m_v+1)}} \tag{16}$$

where x is burn fraction and it is 0 at the beginning of the combustion and becomes 1 at the end of the combustion. It can be rewritten by differentiating with respect to crank angle:

$$\frac{dx}{d\theta}=a_v\left(\frac{\theta}{\theta_b}\right)^{m_v}\left(\frac{m_v+1}{\theta_b}\right)e^{-a_v\left(\frac{\theta}{\theta_b}\right)^{(m_v+1)}} \tag{17}$$

$$\theta=\theta_r-\theta_s \tag{18}$$

where θ_r and θ_s are reference crank angle and start angle of combustion respectively, a_v, m_v are Wiebe constants combustion process and θ_b is combustion duration in crank angle.

NO emissions are calculated by using extended Zeldovich mechanism taking into account 10 combustion products including (CO_2, H_2O, N_2, O_2, CO, H_2, H, O, OH, NO) [20]. In this study the ECP code which is developed by Olikara and Borman [21] is modified by adding steam injection into the reactants. The combustion reaction used in the modified program is given below:

$$\varepsilon\phi C_\alpha H_\beta O_\gamma N_\delta+(0.21O_2+0.79N_2)+zH_2O\rightarrow \nu_1CO_2+\nu_2H_2O+\nu_3N_2+\nu_4O_2+\nu_5CO+\nu_6H_2+\nu_7H+\nu_8O+\nu_9OH+\nu_{10}NO \tag{19}$$

The z in the reactants is mole fraction of injected steam and can be calculated as:

$$x=\frac{Y_{\%}M_f}{M_{ste}} \tag{20}$$

where M_f and M_{ste} are molecular weights of the fuel and steam. $Y_{\%}$ is ratio of the steam mass to the fuel mass and defined as:

$$Y_{\%}=\frac{m_{ste}}{m_f} \tag{21}$$

The rate constant is expressed as:

$$k=A_AT^{B_A}e^{\frac{E_A}{T}} \tag{22}$$

The rate of NO formation [mol cm^{-3} s^{-1}] is

$$\frac{d[NO]}{dt}=\frac{2R_1\left(1-\alpha^2\right)}{1+\frac{\alpha R_1}{R_2+R_3}} \tag{23}$$

where $\alpha=[NO]/[NO]_e$ and $[]_e$ denotes equilibrium concentration. The other constants used in Eq. (23) are;

$$R_1=k_{+1}[N_2]_e[O_2]_e=k_{-1}[NO]_e[N]_e \tag{24}$$

$$R_2=k_{+2}[O_2]_e[N]_e=k_{-2}[NO]_e[O]_e \tag{25}$$

$$R_3=k_{+3}[OH]_e[N]_e=k_{-3}[NO]_e[H]_e \tag{26}$$

3. Results and discussion

In the study, the steam was injected at different mass ratios of fuel (%10, 20 and 30), into intake manifold when intake valves were opened during the suction period. From the experimental results, optimum steam ratio was determined as 20% (S20) in terms of engine performance. Fig. 3 shows the comparison of theoretical and experimental data of brake torques. The experimental results obtained in terms of engine performance and emissions are given in comparison with the results of zero-dimensional-two-zone combustion model for 20% steam ratio.

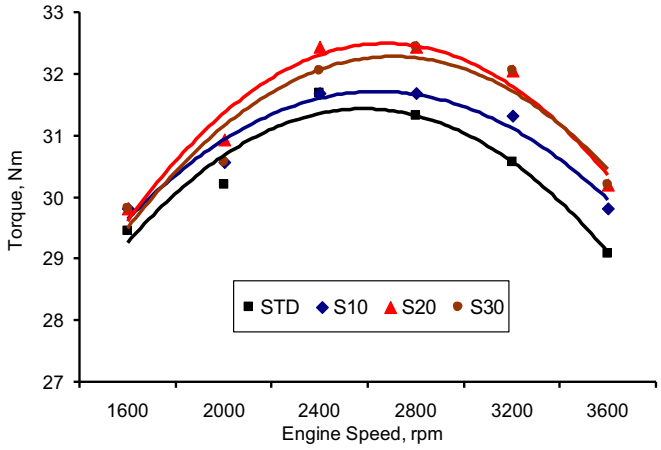

Fig. 3. The variation of engine torque with respect to engine speed at different modes.

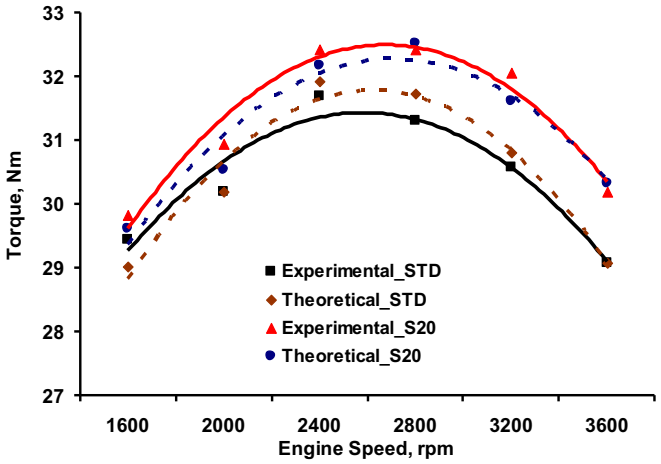

Fig. 5. Comparison of theoretical and experimental data of torque.

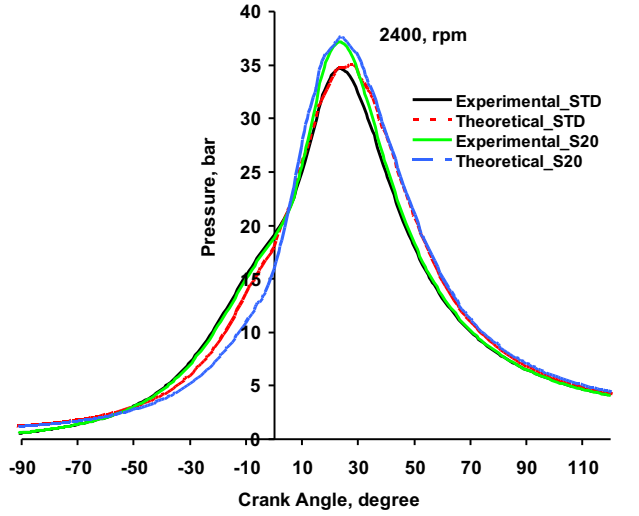

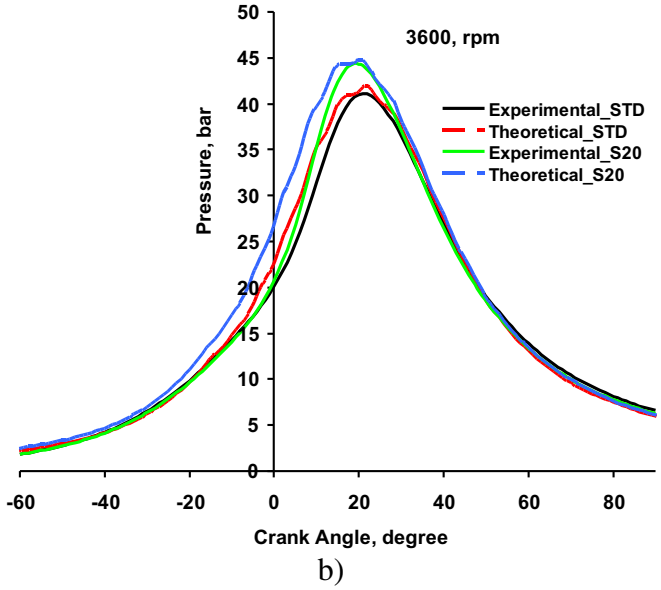

Fig. 4. Comparison of theoretical and experimental data for cylinder pressures.

3.1. In-cylinder pressure

Fig. 4 shows the comparison of in-cylinder pressures of theoretical and experimental data with 20% steam ratio at full-load conditions. It is seen that the values of theoretical combustion model developed are very close to the actual values. The figure shows that the engine working with S20 consumes lower work during compression and produces higher work during expansion period. This is the main reason why the engine running with S20 produces more power and brakes torque according to standard SI engine. During compression, finer steam droplets contribute better air-fuel mixing and cause to decrease the compression temperature and pressure in the cylinder as steam absorbs more heat. The figure also shows pressure gradient of the engine running with S20 sharply increases compare to standard SI engine after the TDC. This may be explain with the reason that steam shortens combustion duration after TDC.

3.2. Engine torque

Fig. 5 shows the comparison of the theoretical and experimental data for variation of engine torques at the condition of 20% steam injection. As can be seen from the figure, torque increases at all engine speeds. While the maximum torque reached is 32.43 Nm at 2400 rpm at 20% steam injection rate, it is 31.68 Nm at standard

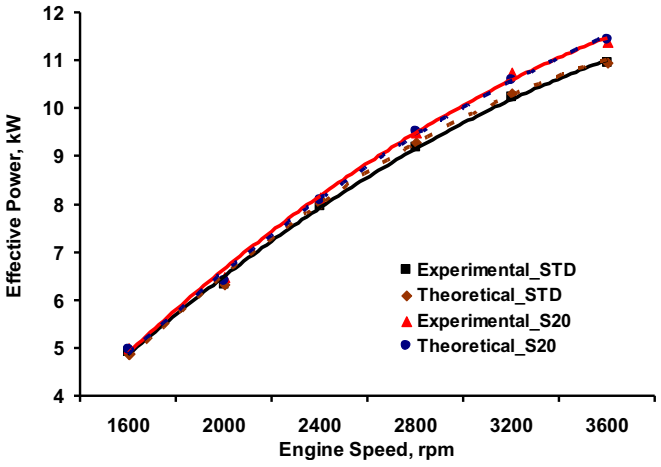

Fig. 6. Comparison of theoretical and experimental data of effective power.

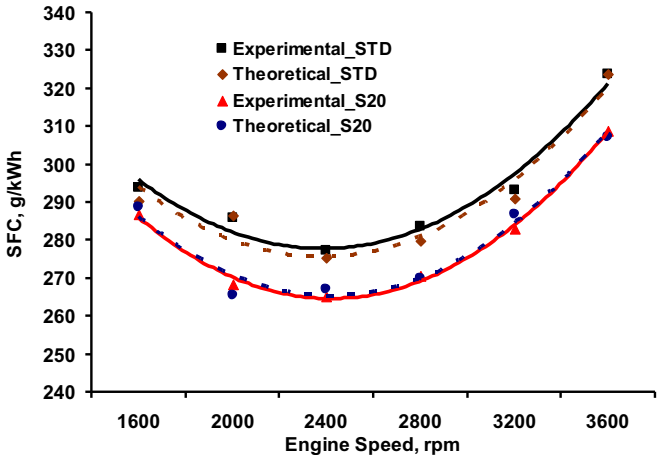

Fig. 7. Comparison of theoretical and experimental data of SFC.

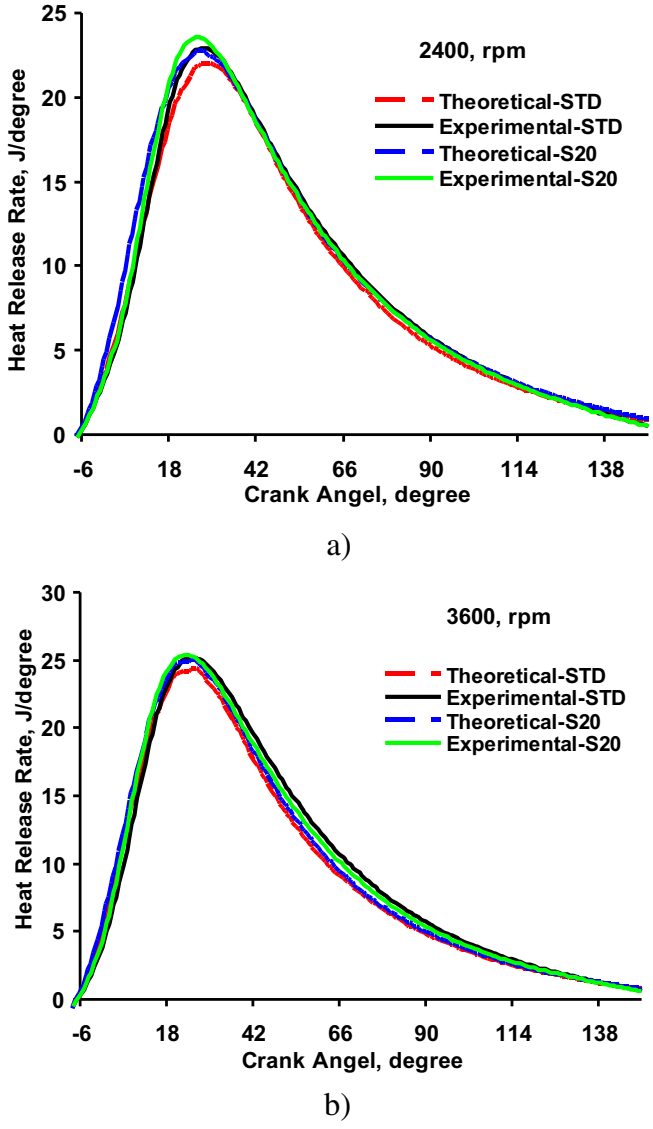

Fig. 8. Comparison of theoretical and experimental data for heat release rates.

condition. It is seen from the figure that the highest increase in torque is 4.65% at 3200 rpm, the lowest improvement is 1.25% at 1600 rpm.

Based on the previous literature reviews, It can be said that the reason of this improvement is owing to the enthalpy increase and better atomization is carried out with injected steam into the cylinder.

3.3. Effective power

The comparison of the theoretical and experimental results of effective power is illustrated in Fig. 6. As it is observed from the figure, effective power also increases at all engine speeds with S20. As the maximum effective power with steam injection is 11.37 kW at 3600 rpm, it is 10.96 kW at 3600 rpm in standard condition. According to standard effective power values, the peak change is 4.65% at 3200 rpm, the minimum change is 1.25% at 1600 rpm.

3.4. Specific fuel consumption

The theoretical and experimental data of specific fuel consumption (SFC) is indicated in Fig. 7 comparatively. It is seen from the figure that SFC reduces at all engine speeds with S20. The lowest SFC is 265.07 g/kWh at 2400 rpm. As the maximum reduction is 6.4% at 2000 rpm, the lowest change is 2.43% at 1600 rpm when compared to standard SFC.

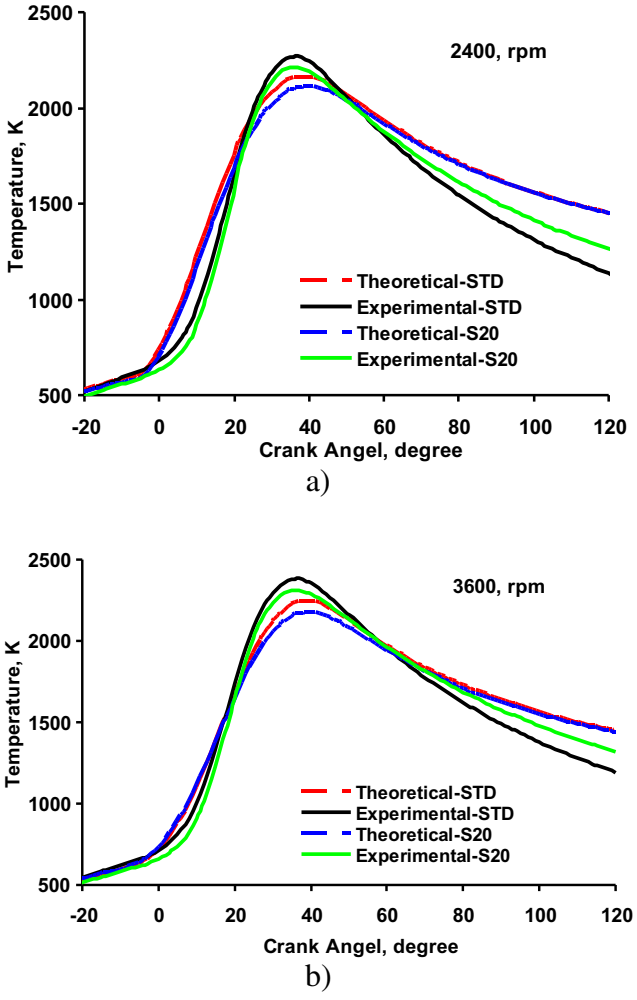

Fig. 9. Comparison of theoretical and experimental data for in-cylinder temperatures.

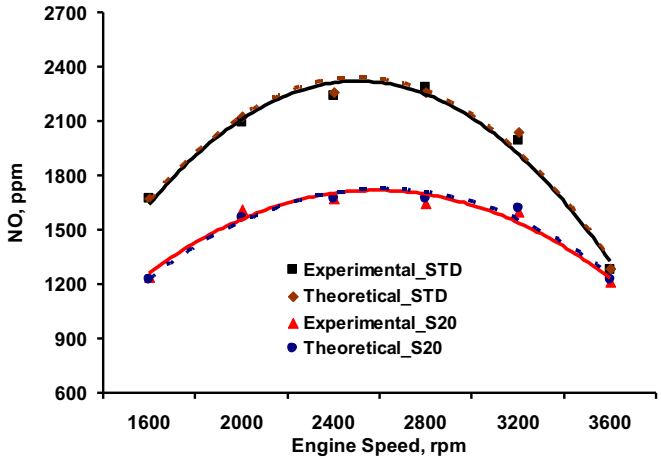

Fig. 10. Comparison of theoretical and experimental data of NO emission.

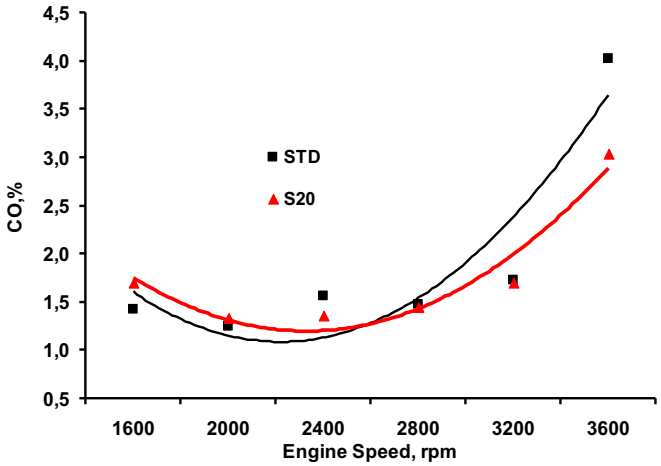

Fig. 12. The effect of steam injection on the variation of CO emission.

3.5. Exhaust emissions

3.5.1. Heat release rates, in-cylinder temperatures and NO formation

The heat release rate figures are illustrated in Fig. 8a–b. The peak heat release rate of the steam injected engine is higher than that of standard engine.

Fig. 9a–b shows the comparison of in-cylinder temperatures at full-load conditions with respect to engine speed. It is clear that NO formation rate strongly depends on peak temperature and duration of combustion at peak temperature in the cylinder [22]. Hence, when the steam is injected into cylinder, peak temperatures decreased compared to that of standard SI engine.

Fig. 10 illustrates the comparison of theoretical and experimental data of NO emissions. As can be seen from the figure, steam injection leads to reduce NO emissions as the maximum combustion temperatures decrease. While the maximum NO emission with steam injection is 1722 ppm at 2000 rpm, it is 2091 ppm at standard condition. The maximum and minimum reductions are 40% at 2800 rpm and 5% at 3600 rpm, respectively.

The interest in water injection techniques is due to the fact that water in the form of micrometer sized droplets exerts some positive effects on the combustion of the fuel and exhaust emissions, frequently NO_x. Steam injection to SI engines also showed same positive effects with water injection techniques, such as reduced NO_x and improved combustion efficiency. It can be concluded that the finely atomized droplets are mixed with air instantly and more homogenously after being injected into the combustion chamber. The combined effect of vaporization absorbing heat, relatively high molar heat capacity of water and increased partial pressure of oxygen puts down the peak combustion temperature and thus decreases the nitrogen oxides formation [23,24].

3.5.2. HC emissions

The comparison of HC emissions of steam injected and standard SI is indicated in Fig. 11. The HC emissions decrease with steam injection at all engine speeds. As the maximum HC emission is 302 ppm at steam injected condition, it is 377 ppm in standard condition. The maximum and minimum reductions are 31.5% at 2000 rpm and 21.93% at 2800 rpm, respectively.

The reduction in HC with S20 could be explained owing to the presence of the fuel–steam interface with very low interfacial tension which causes to a better atomization of the fuel during injection. Higher contact with the air during the burning process is resulted in a finer dispersion of the fuel droplets [12,23]. Another possible reason reducing in HC may be explained with the improvement in vaporization and mixing processes which leads to a shorter combustion reaction [12,22].

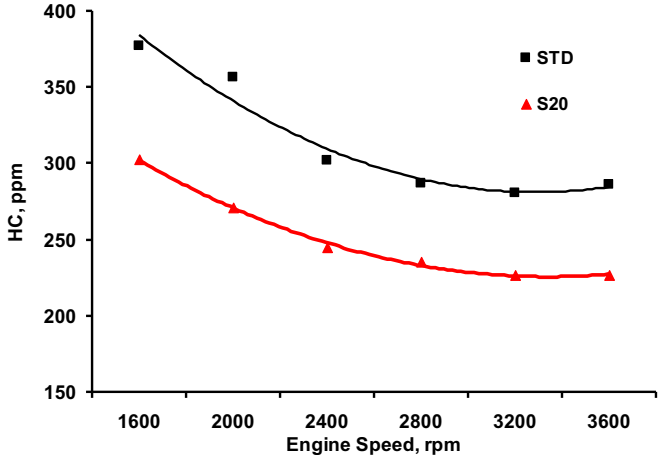

Fig. 11. The effect of steam injection on the variation of HC emission.

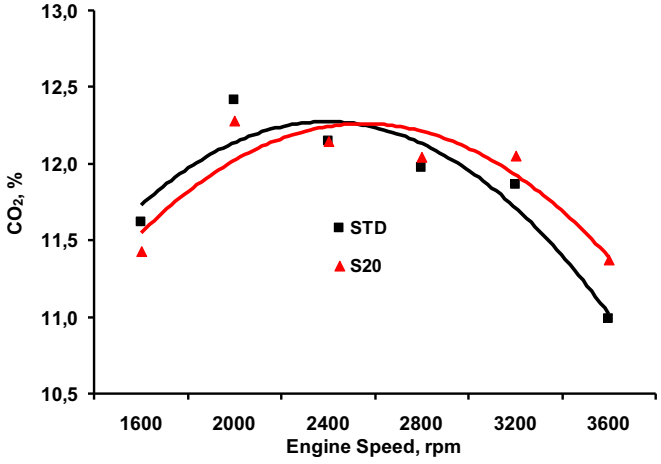

Fig. 13. The effect of steam injection on the variation of CO_2 emission.

3.5.3. CO and CO_2 emissions

Fig. 12 shows the comparison of CO emissions of steam injected and standard SI engines. While the CO emissions enhance with steam injection at lower engine speeds (1600–2000 rpm), a reduction is observed at higher engine speeds (2400–3600). The minimum CO emission is 0.35% at 2400 rpm in comparison to standard condition. The comparison of CO_2 emissions of steam injected and standard SI engine is illustrated in Fig. 13. Contrarily, as CO_2 emissions diminish at lower engine speeds, it increases at higher engine speeds.

4. Conclusion

In this study, the effects of electronically controlled steam injection system developed by Parlak et al. [14,15] on performance and emissions have been investigated and modeled by zero-dimensional two-zone combustion model. When compared with experimental and theoretical data, torque, effective power and efficiency, SFC and NO emissions were agree with actual values with 1.47% maximum error.

In the study, an improvement is observed in torque and effective power and SFC with steam injection and NO and HC emissions decrease significantly. The maximum torque was obtained at 2400 rpm at 20% steam injection which is optimum rate. The maximum change in torque and power has been determined at 3200 rpm as 4.65%. Furthermore, maximum power has been obtained at 3600 rpm. Whilst minimum SFC has been obtained at 2400 rpm, the highest change in SFC is at 2000 rpm.

As the maximum NO is 2091 ppm at 2000 rpm and standard condition, it occurs 1722 ppm at steam injected condition. The maximum change in NO emissions has been determined at 2800 rpm as 40%. In HC emissions it is 31.5% at 2000 rpm.

It is clear that this study could be used by the real-engine designers by considering the effects of steam injection into the gasoline engine cylinder.

Acknowledgements

This work has been supported by The Scientific and Technological Research Council of Turkey and was performed within The Support Programme for Scientific and Technological Research Projects (1001) with the project number of 111M056 and Scientific and Technological Research Projects of Sakarya University.

References

[1] Y. Wang, L. Lin, A.P. Roskilly, S. Zeng, J. Huang, Y. He, X. Huang, H. Huang, H. Wei, L.S. Shangping, J. Yang, An analytic study of applying Miller cycle to reduce NO_x emission from petrol engine, Applied Thermal Engineering 27 (2007) 1779–1789.
[2] J.P. Melo, A.M. Mellor, NO_x emissions from direct injection diesel engines with water/steam dilution, SAE Technical Papers (1999), 1999-01-0836.
[3] M. Christensen, B. Johansson, Homogeneous charge compression ignition with water injection, SAE Technical Papers (1999), 1999-01-0182.
[4] K.P. Duffy, A.M. Mellor, Further developments on a characteristic time model for NO_x emissions from diesel engines, SAE Technical Papers (1998), 982460.
[5] F.L. Drayer, Water addition to practical combustion systems – concepts and application, in: 16th Symposium on Combustion, Combustion Institute, Cambridge, MA, Aug. 1976.
[6] C.A. Canfield, Effects of Diesel–Water Emulsion Combustion on Diesel Engine NO_x Emission, Master of Science, University of Florida, 1999.
[7] A. Lif, K. Holmberg, Water-in-diesel emulsions and related systems, Advances in Colloid and Interface Science (2006) 231–239.
[8] Y. Yoshimoto, M. Tsukaara, T. Kuramoto, Improvements of BSFC by reducing diesel engine cooling losses with emulsified fuel, SAE Technical Papers (1996), 962022.
[9] X. Hang, O.S. Yunbai, Z. Chongji, M. Yuanji, in: Proceeding of the 5th International Conference on Liquid Atomization and Spray Systems, Natl Inst of Standards and Technology, Gaithersburg, MD, USA, 1991, p. 307.
[10] R. Lanzafame, Water injection effects in a single-cylinder CFR engine, SAE Technical Papers (1999), 1999-01-0568.
[11] V. Subramanian, J.M. Mallikarjuna, A. Ramesh, Effects of water injection and spark timing on the nitric oxide emissions and combustion parametres of a hydrogen fuelled spark ignition engine, International Journal of Hydrogen Energy 32 (2007) 1159–1173.
[12] V. Ayhan, Investigation of Steam Injection on Performance and Exhaust Emissions of a DI Diesel Engine, Sakarya University, PhD thesis, 2009 (in Turkish).
[13] A. Parlak, V. Ayhan, Y. Üst, B. Şahin, İ. Cesur, B. Boru, G. Kökkülünk, New method to reduce NO_x emissions of diesel engines: electronically controlled steam injection system, Journal of the Energy Institute 85 (2012) 135–139.
[14] A. Parlak, V. Ayhan, B. Şahin, İ. Cesur, B. Boru, G. Kökkülünk, The effects of the new developed electronic controlled steam injection system on NO_x emissions of a single cylinder diesel engine, in: 13th International Conference Maritime Transport and Infrastructure, Riga, 2011.
[15] G. Kokkulunk, A. Parlak, V. Ayhan, G. Gonca, Theoretical and experimental investigation of diesel engine with steam injection system on performance and emission parameters, Applied Thermal Engineering 54 (1) (2013) 161–170.
[16] R. Ferguson, Internal Combustion Engines – Applied Thermodynamic, John Wiley & Sons, New York, 1986.
[17] A. Safa, Process and Emission Modeling in the Internal Combustion Engines, Ph.D. thesis, YTU Graduate School of Natural and Applied Sciences Istanbul, 2006 (in Turkish).
[18] G.F. Hohenberg, Advanced approaches for heat transfer calculation, SAE Technical Papers (1979).
[19] N. Miyamoto, T. Chikahisa, T. Murayama, R. Sawyer, Description and analysis of diesel engine rate of combustion and performance using Wiebe's functions, SAE Technical Paper Series (1985) 0107.
[20] G.L. Borman, K.W. Ragland, Combustion Engineering, McGraw-Hill Book Company, Boston, 1998.
[21] C. Olikara, G. Borman, A computer program for calculating properties of equilibrium combustion products with some applications to the engines, SAE Technical Paper Series (1975) 0468.
[22] J.B. Heywood, Internal Combustion Engine Fundamentals, McGraw-Hill Inc., New York, 1998.
[23] C.Y. Lin, K.H. Wang, Effects of diesel engine speed and water content on emission characteristics of three-phase emulsions, Journal of Environmental Science and Health Part A 39 (5) (2004) 1345–1359.
[24] J.W. Park, K.Y. Huh, K.H. Park, Experimental study on the combustion characteristics of emulsified diesel in a rapid compression and expansion machine, Proceedings of the Institution of Mechanical Engineers Part D 214 (2000) 579–586.